

First-principles studies of water adsorption on graphene: The role of the substrate

Tim O. Wehling,^{1,*} Mikhail I. Katsnelson,² and Alexander I. Lichtenstein¹

¹*I. Institut für Theoretische Physik, Universität Hamburg, Jungiusstraße 9, D-20355 Hamburg, Germany*

²*Institute for Molecules and Materials, Radboud University of Nijmegen, Heijendaalseweg 135, 6525 AJ Nijmegen, The Netherlands*

(Dated: October 25, 2018)

We investigate the electronic properties of graphene upon water adsorption and study the influence of the SiO₂ substrate in this context using density functional calculations. Perfect suspended graphene is rather insensitive to H₂O adsorbates, as doping requires highly oriented H₂O clusters. For graphene on a defective SiO₂ substrate, we find a strongly different behavior: H₂O adsorbates can shift the substrate's impurity bands and change their hybridization with the graphene bands. In this way, H₂O can lead to doping of graphene for much lower adsorbate concentrations than for free hanged graphene. The effect depends strongly on the microscopic substrate properties.

Graphene, i.e. a monolayer of graphite, is the first truly two dimensional (2D) material [1, 2] and a promising candidate for silicon replacement in semiconductor industry [3] or gas sensing applications [4, 5]. Since graphene's discovery the water adsorbates have been discussed as impurities leading to doping [1, 4], while changing the electron mobility in graphene only surprisingly little. Up to now, the microscopic mechanism of this doping without significant changes in electron mobility has remained unclear. Density functional theory calculations on single water molecule adsorbates on perfect free standing graphene [6] were in line with previous studies on carbon nanotubes (CNT) [7] and found H₂O physisorption but no H₂O induced impurity states close to the Fermi level. Therefore, the doping effects found experimentally [1, 4] are very likely due to more complicated mechanisms than interactions of graphene with single water molecules. The experiments dealing with the effect of water on graphene were carried out using graphene on top of SiO₂ substrates. In addition, for finite concentrations of H₂O on graphene H₂O clusters might form. Despite its importance for understanding the doping experiments [1, 4] and for possible graphene based applications, a microscopic theory on the role of the substrate and H₂O-clusters in the H₂O-graphene-interplay has been lacking, so far.

In this letter we study the substrate and cluster formation effects in the water-graphene-system by means of density functional theory (DFT). We show that both, highly oriented water clusters as well as water adsorbates in combination with a defective SiO₂ substrate can lead to doping of graphene. To this end, we consider model systems (see Fig. 1) for water and ice in different concentrations of free standing graphene as well as for water interacting with defective SiO₂ substrates. By analyzing the involved dipole moments and comparison to electrostatic force microscopy [8], we show that the SiO₂ substrate is crucial for obtaining doping by H₂O adsorbates on graphene.

In our DFT calculations, the electronic and structural properties of the graphene-substrate-adsorbate systems

are obtained using generalized gradient approximation (GGA)[9, 10] to the exchange correlation potential. For solving the resulting Kohn-Sham equation we used the Vienna Ab Initio Simulation Package (VASP) [11] with the projector augmented wave (PAW) [12, 13] basis sets implemented, there. The graphene-substrate-adsorbate systems are modeled using supercells containing up to 83 substrate atoms (Si, O and H), 12 adsorbate atoms and 32 C atoms.

Firstly, water adsorption on free standing graphene with different water concentrations is considered. To model a single H₂O molecule on graphene, 3 × 3 graphene supercells were used. Full relaxation of H₂O with oxygen or hydrogen nearest to the graphene yielded adsorbed configurations with binding energies of 40 meV and 36 meV and molecule sheet distances of 3.50 Å and 3.25 Å, respectively. These values are in the same order as those obtained by Leenaerts et. al. [6] indicating physisorption of single water molecules on graphene. Analyzing the density of states/band structures for these two adsorption geometries we find qualitative agreement with Ref. [6]: None of these configurations exhibits energy levels due to the adsorbate near the Dirac point, as shown in Fig. 2 a) for the configuration with oxygen closest to graphene. The HOMO of H₂O is more than 2.4 eV below the Fermi energy and its LUMO more than 3 eV above it. The absence of any additional impurity level close to the Dirac point shows that single water molecules on perfect free standing graphene sheets do not cause any doping.

The supercell applied here, corresponds to an adsorbate concentration of $n = 2 \text{ nm}^{-2}$, which is well inside the range of concentrations (1-10 nm⁻²) found experimentally in Ref. [8]. The lateral dimension $a = 4.5 \text{ Å}$ of the hexagonal ice Ih (0001)-surface unit cell corresponds to a concentration of 5.7 H₂O nm⁻² per layer. Thus, increasing the H₂O concentration significantly above the $n = 2 \text{ nm}^{-2}$ from above leads to water clusters or ice like structures, rather than isolated molecules.

To gain insight into doping of graphene by water clusters and ice overlayers we studied fully relaxed bi-layers and four layers of ice Ih adsorbed on graphene. These

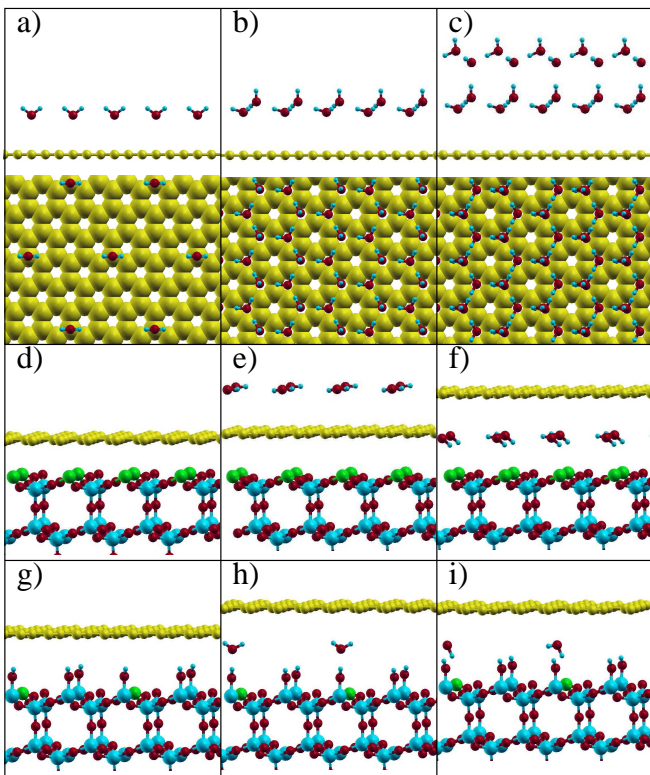


Figure 1: (Color online) Model systems for water interacting with graphene. a-c: Free standing graphene with single water adsorbates (a), a bilayer (b) and a tetralayer (c) of ice Ih. Carbon atoms yellow, oxygen red and hydrogen small blue balls. d-i: graphene on top of SiO₂ with every second (d-f) or eighth (g-i) surface Si atom forming a Q₃⁰ defect. Water adsorbates are considered on top of graphene (e), and between graphene and the substrate (f), (h), and (i). Fully coordinated Si atoms are depicted as big blue balls, Si atoms at Q₃⁰ defects in green.

overlayer structures have been proposed as basis of ice growth on various hexagonal metal surfaces [14, 15] and can be modeled as $(\sqrt{3} \times \sqrt{3})R30^\circ$ overlayer on the simple graphene unit cell. The lattice mismatch in this configuration is 0.23 \AA — on the same order as found for water overlayers on Ni(111) [14] — and therefore a reasonable starting point for studying ice on graphene.

The supercell bandstructures (Fig. 2 b) and c)) show that the electric field by proton-ordered ice on top of graphene changes the energy of graphene’s nearly free electron bands. In contrast to pristine graphene, where these bands start at 3eV above the Dirac point or in the case of single H₂O adsorbates on graphene (Fig. 2 a)), their bottom is at 0.6eV above and 0.1eV below the Dirac point for a bi- and a tetralayer of ice Ih on top of graphene. This shift is due to electrostatic fields induced by the H₂O dipole moments and results in hole doping for the tetralayer of ice on graphene.

The water adlayers cause a change in contact potential $\delta\phi$, which can be estimated using the H₂O dipole mo-

ment $p = 6.2 \times 10^{-30} \text{ Cm}$ and the relaxed structures to be $\delta\phi = 1.4\text{V}$ and 5.4V for a water bi- and tetralayer, respectively. While only the latter structure causes doping, the corresponding change in contact potential exceeds the experimental value, $p_{\text{exp}} = 1.3\text{V}$, from Ref. [8] by more than a factor of 4. However, water strongly diluted in N₂ has been found to cause hole doping in graphene on SiO₂[4]. Given these two experiments, doping due to multiple fully oriented ice overlayers as in Fig. 2 is likely not the most important interaction mechanism for water and graphene.

We now turn to studying the effect of the SiO₂ substrate in the water-graphene interplay. The experiments with graphene on top of SiO₂ used substrates, which were created by plasma oxidation of Si. [4, 8] The SiO₂ surface created in this way is amorphous and its electronic, structural and chemical properties are challenging to model from first principles. To obtain, qualitative insight to the most important physical mechanisms it is, however, a reasonable starting point to consider crystalline SiO₂ in the β -cristobalite form as a substrate [16].

The (111) surface of this modification can be used to create the most likely defects on SiO₂ amorphous surfaces: These are so called Q₃⁰ and Q₄¹ defects [17] having one under coordinated silicon and oxygen atom, respectively. Furthermore, the unit cell of this surface is nearly commensurate with the graphene lattice: The lattice constant $a_{\text{SiO}_2} = 7.13 \text{ \AA}$ [18] results in a surface unit cell $a_{\text{SiO}_2}/\sqrt{2} = 5.04 \text{ \AA}$, which is 4% larger than twice the lattice constant $2a_0 = 4.93 \text{ \AA}$ of graphene. As the SiO₄ tetrahedra in SiO₂ are known to adjust to external strain easily, we model graphene on SiO₂ by 2×2 or 4×4 graphene supercells with lateral dimension $2a_0$ or $4a_0$. As substrate we put 4% laterally strained and hydrogen passivated β -cristobalite with 6 Si atoms per surface unit cell in vertical direction. We then created the defects by removing H passivation atoms, added the H₂O adsorbates and relaxed until all forces were less than $0.08 \text{ eV} \cdot \text{ \AA}^{-1}$. In this way, we consider passivated and defective SiO₂ surfaces — the latter containing either undercoordinated silicon or oxygen atoms — as substrate for graphene. The effect of water exposure is simulated by putting water molecules on top of graphene as well as between graphene and the substrate.

Graphene on top of fully passivated SiO₂ means two inert systems in contact with each other. Consequently, there are no bands in addition to graphene’s Dirac bands at the Fermi level and no doping occurs. (The band structure is not shown here, for brevity.) This changes strongly for graphene on defective SiO₂. As a model system, we study Q₃⁰ defects in β -cristobalite (111)-surfaces. Depending on the supercell size, 2×2 and 4×4 , in these periodic structures every second and eighth surface Si atom is under coordinated, respectively, and forms a Q₃⁰ defect. (See Fig. 1 (d-i).)

These defects lead to additional states in the vicinity

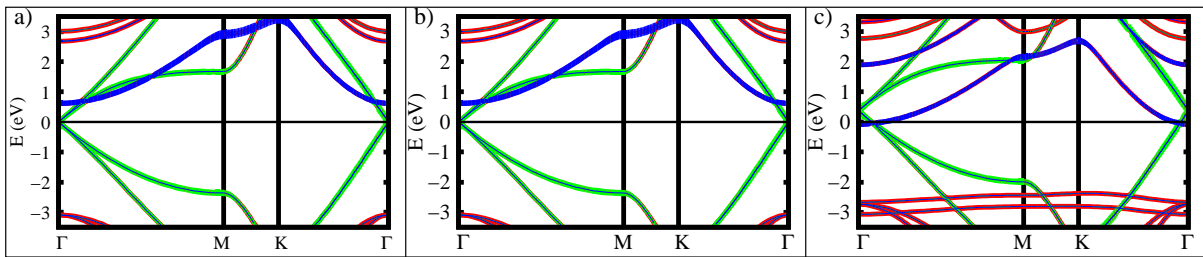


Figure 2: (Color online) Bandstructures of supercells with fully relaxed single molecules (a), a bilayer (b) and a tetralayer (c) of water on graphene, corresponding to Fig. 1 a-c), respectively, are shown. The graphene π bands are marked in green, the nearly free electron bands in blue. Due to the H_2O dipole moments, graphene's nearly free electron band is shifted with respect to its π bands.

($\pm 1\text{eV}$) around the Fermi level. (See Fig. 3 a) and d).) The avoided crossing in Fig. 3 a) indicates significant hybridization of the defect and the graphene bands and demonstrate the impurity state's importance for conduction electron scattering in graphene. In the pure SiO_2 graphene model systems (Fig. 3 a) and d)), the impurity bands do not cross the Fermi level. This situation can be changed by water adsorbates, which may sit either in between graphene and the substrate (Fig. 3 c), e) and f) or on top of graphene (Fig. 3 b)). In all cases, the electrostatic dipole moment of the water adsorbates comes along with strong local electrostatic fields, which allow to shift the impurity bands significantly with respect to the graphene bands. As Fig. 3 demonstrates, this shift strongly depends on the place of adsorption and the orientation of the water molecules leading, either to hole doping (Fig. 3 c) and f)) or electron doping (Fig. 3 e)).

This strong effect of water is very general and not limited to the examples shown in Fig. 3. Similar effects of water can be found for graphene on the (0001)-plane of α -quartz or β -cristobalite with Q_4^1 defects. Although the interaction mechanisms of water, SiO_2 and graphene presented here are not exhaustive, the comparison of water adsorption on perfect free standing graphene to water adsorption on graphene lying on a (defective) SiO_2 substrate allows the following conclusions: Perfect free standing graphene may have water adsorbates on top but its electronic transport properties are insensitive against perturbations by the water adsorbates. Single molecules will not create any impurity states close to the Dirac point. For obtaining doping effects, one needs highly ordered H_2O cluster or ice structures.

The substrate changes the situation completely. The dipole moments of H_2O adsorbates cause local electrostatic fields that can shift the substrate's defect states with respect to the graphene electrons and cause doping. The hybridization of substrate defect states with the graphene bands can be reduced by H_2O in between graphene and the substrate leading to less scattering of graphene electrons at defects in the substrate. On the other hand, impurity bands can be shifted towards the

Fermi level by H_2O adsorbates, leading to increased electron scattering. So, for graphene on a substrate, H_2O much more likely affects the electronic properties than for free standing graphene. The effect of water strongly depends on properties of the substrate like the amount and type of defects.

This finding might explain experiments on CNTs [19]: CNTs on SiO_2 substrates are much more sensitive to water in their environment, than suspended CNTs or CNTs separated from the SiO_2 substrate by poly(methyl methacrylate) (PMMA) coating. In experiments similar to those in Refs. [3, 20] these effects can be checked for graphene: The creation of electron/hole puddles and doping on H_2O exposure might be investigated in a study with a similar setup as in Ref. [20]. We expect much less impact of H_2O on the transport properties for free hanged graphene. Similarly, a comparison of graphene on hydrophobic substrates and hydrophilic substrates like PMMA and SiO_2 in Ref. [3] should yield weak and strong response on H_2O , respectively.

These findings can be important for the development of graphene based gas sensing devices: Some molecules like NO_2 lead to acceptor states even without a substrate [5], while doping effects due to other molecules like H_2O strongly depend on the substrate. This can open the possibility of selective graphene gas sensors.

The authors are thankful to Andre Geim and Kostya Novoselov for inspiring discussions. This work was supported by SFB 668 (Germany) and FOM (The Netherlands). Computation time at HLRN is acknowledged.

* Electronic address: twehling@physnet.uni-hamburg.de

- [1] K. S. Novoselov, A. K. Geim, S. V. Morozov, D. Jiang, Y. Zhang, S. V. Dubonos, I. V. Grigorieva, and A. A. Firsov, *Science* **306**, 666 (2004).
- [2] K. S. Novoselov, D. Jiang, F. Schedin, T. J. Booth, V. V. Khotkevich, S. V. Morozov, and A. K. Geim, *PNAS* **102**, 10451 (2005).
- [3] S. V. Morozov, K. S. Novoselov, M. I. Katsnelson, F. Schedin, D. C. Elias, J. A. Jaszczak, and A. K. Geim,

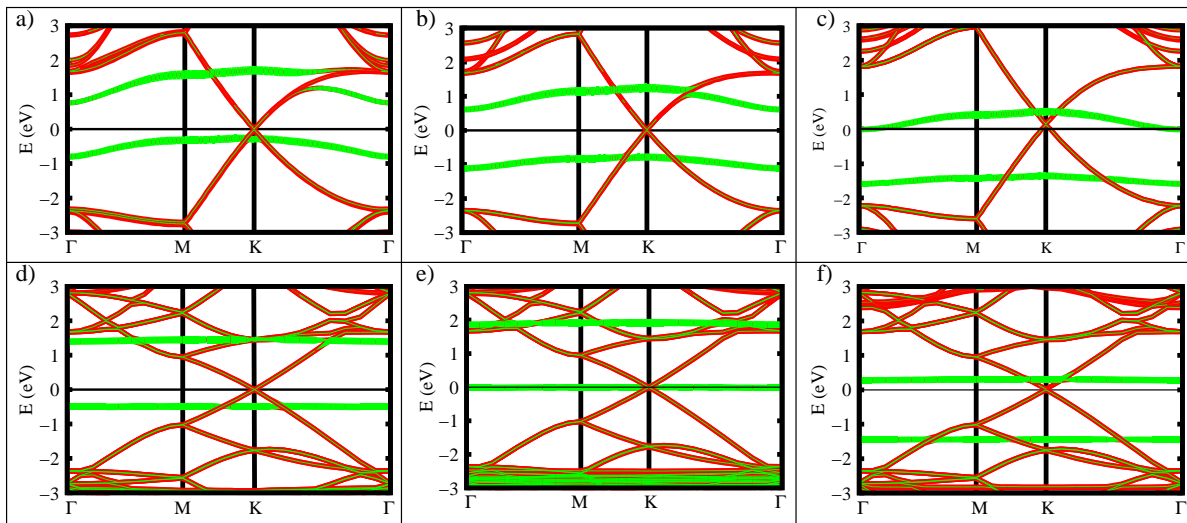


Figure 3: (Color online) Band structures for graphene on defective SiO_2 substrates. (a-c) 2×2 and (d-f) 4×4 graphene supercells with every second, (a-c), or eighth, (d-f) surface Si atom forming a Q_3^0 defect. The corresponding geometries are shown in Fig. 1 d-i), respectively. Spin up and down bands are shown at the same time. Contributions at the defect site are marked as green fatbands. a) and d) without water adsorbates. b) with water on top of graphene. c), e), and f) with water between graphene and the substrate. c), f) H_2O dipole moment pointing tilted downwards. e) H_2O dipole moment pointing upwards.

- Phys. Rev. Lett. **100**, 016602 (2008).
- [4] F. Schedin, A. K. Geim, S. V. Morozov, E. W. Hill, P. Blake, M. I. Katsnelson, and K. S. Novoselov, Nat. Mater. **6**, 652 (2007).
- [5] T. Wehling, K. Novoselov, S. Morozov, E. Vdovin, M. Katsnelson, A. Geim, and A. Lichtenstein, Nano Letters **8**, 173 (2008).
- [6] O. Leenaerts, B. Partoens, and F. M. Peeters, Phys. Rev. B **77**, 125416 (2008).
- [7] J. Zhao, A. Buldum, J. Han, and J. P. Lu, Nanotechnology **13**, 195 (2002).
- [8] J. Moser, A. Verdaguer, D. Jimenez, A. Barreiro, and A. Bachtold, Appl. Phys. Lett. **92**, 123507 (2008).
- [9] J. P. Perdew, J. A. Chevary, S. H. Vosko, K. A. Jackson, M. R. Pederson, D. J. Singh, and C. Fiolhais, Phys. Rev. B **46**, 6671 (1992).
- [10] J. P. Perdew, K. Burke, and M. Ernzerhof, Phys. Rev. Lett. **77**, 3865 (1996).
- [11] G. Kresse and J. Hafner, J. Phys.: Condes. Matter **6**, 8245 (1994).
- [12] P. E. Blöchl, Phys. Rev. B **50**, 17953 (1994).
- [13] G. Kresse and D. Joubert, Phys. Rev. B **59**, 1758 (1999).
- [14] T. Lankau, *A computational analysis of hydrogen-bonded networks*, Department of Chemistry, University of Hamburg (2004), habilitation thesis.
- [15] S. Meng, E. Kaxiras, and Z. Zhang, J. Chem. Phys. **127**, 244710 (2007).
- [16] P. Carrier, L. J. Lewis, and M. W. C. Dharma-wardana, Phys. Rev. B **64**, 195330 (2001).
- [17] M. Wilson and T. R. Walsh, J. Chem. Phys. **113**, 9180 (2000).
- [18] A. Wright and A. Leadbetter, Philos. Mag. **31**, 1391 (1975).
- [19] W. Kim, A. Javey, O. Vermesh, Q. Wang, Y. Li, and H. Dai, Nano Letters **3**, 193 (2003).
- [20] X. Du, I. Skachko, A. Barker, and E. Y. Andrei, Nat. Nano. (2008), doi: 10.1038/nnano.2008.199.